Electronic Supplementary Material (ESI) for ChemComm.

Supplementary Material

^{15}N detected TROSY NMR experiments to study large, disordered proteins in high-field magnets

Abhinav Dubey,[a,b] Thibault Viennet,[a,b] Sandeep Chhabra,[a,b] Koh Takeuchi,[c] Hee-Chan Seo,[a,d] Wolfgang Bermel,[e] Dominique Frueh,[f] Haribabu Arthanari*[a,b]

[a] Cancer Biology, Dana-Farber Cancer Institute, Boston MA, 02215 USA. E-mail: hari_arthanari@hms.harvard.edu

[b] Department of Biological Chemistry and Molecular Pharmacology, Harvard Medical School, Boston MA, 02115 USA.

[c] Graduate School of Pharmaceutical Sciences, The University of Tokyo, Tokyo, 113-0033, Japan.

[d] Department of Molecular Biology, University of Bergen, Bergen 5020, Norway.

[e] Magnetic Resonance Spectroscopy NMR Application, Bruker BioSpin GmbH, 76287 Rheinstetten, Germany.

[f] Department of Biophysics and Biophysical Chemistry, Johns Hopkins University School of Medicine, Baltimore, Maryland 21205, USA.

Supplementary Text

1. Estimating the transverse relaxation rates

We used the following equations[1,2] to estimate the transverse relaxation rates of ^{13}CO, $^{15}N^{H}$-^{1}H decoupled, $^{15}N^{D}$-^{2}H decoupled and $^{15}N^{H}$-TROSY with varying rotational correlation times (**Fig 1a**) and magnetic field strengths (**Fig 1b**).

$$R_{2A} = \frac{p}{2}\{4J(0) + J(\omega_A - \omega_B) + 6J(\omega_B) + 3J(\omega_A) + 6J(\omega_A + \omega_B)\} + c_A\left\{\frac{2}{3}J(0) + \frac{1}{2}J(\omega_A)\right\} + \rho_T \quad (1)$$

$$R_{TA} = R_{2A} + \frac{c_B}{2}J(\omega_B) + \frac{1}{2}R_{1B} - \aleph_{DD,CSA}\{4J(0) + 3J(\omega_A)\} \quad (2)$$

$$R_{1B} = p\{J(\omega_A - \omega_B) + 3J(\omega_B) + 6J(\omega_A + \omega_B)\} + \rho_L \quad (3)$$

$$J(\omega) = \frac{2}{5}\frac{\tau_c}{1 + (\omega\tau_c)^2} \quad , \qquad \omega_{A,B} = \gamma_{A,B}B_0$$

$$p = \frac{1}{4}\left(\frac{\mu_0\gamma_A\gamma_B}{4\pi r^3_{A,B}}\frac{h}{2\pi}\right)^2, c_{A,B} = \frac{1}{3}\left(\omega_{A,B}\Delta_{A,B}\right)^2, \aleph_{DD,CSA} = 2\frac{\mu_0\gamma_A\gamma_B\omega_A\Delta_A}{48\pi r^3_{A,B}}\frac{h}{2\pi}$$

$$\rho_L = \sum_{i=1}^{N} p_i\{J(\omega_{Ci} - \omega_B) + 3J(\omega_B) + 6J(\omega_{Ci} + \omega_B)\}$$

$$\rho_T = \sum_{i=1}^{M} \frac{p_i}{2}\{4J(0) + J(\omega_A - \omega_{Di}) + 6J(\omega_{Di}) + 3J(\omega_A) + 6J(\omega_A + \omega_{Di})\}$$

where B_O is the magnetic field strength, γ is the gyromagnetic ratio, τ_c is the rotational correlation time, R_{2A} is the transverse relaxation rate of spin A, R_{TA} is the transverse relaxation rate of TROSY spin state of spin A, R_{1B} is the longitudinal relaxation rate of spin B, h is Planck's constant, μ_0 is permeability of the free space, Δ is the chemical shift anisotropy.

a) *Estimating transverse relaxation rate of ^{13}CO:* Equation (1) was used where $^{13}CO_i$ is spin A and directly bonded $^{15}N_i$ as spin B. The dipole-dipole relaxation contribution in ρ_T is from (spin D) $^{1}H_i^N$, $^{1}H_{i-1}^N$, $^{1}H_i^\alpha$, $^{13}C_i^\alpha$.

b) *Estimating transverse relaxation rate of $^{15}N^H$:* Equation (1) was used where $^{15}N_i$ is spin A and directly bonded $^{1}H_i^N$ as spin B. The dipole-dipole relaxation contribution in ρ_T is from (spin D) $^{13}CO_i$, $^{1}H_i^\alpha$, $^{13}C_i^\alpha$.

c) *Estimating transverse relaxation rate of $^{15}N^D$:* Equation (1) was used where ^{15}N is spin A and directly bonded $^{2}H^N$ as spin B. The dipole-dipole relaxation contribution in ρ_T is from (spin D) $^{13}CO_i$, $^{1}H_i^\alpha$, $^{13}C_i^\alpha$.

d) *Estimating transverse relaxation rate of $^{15}N^{TROSY}$:* Equations (2) and (3) were used where $^{15}N_i$ is spin A and directly bonded $^{1}H_i^N$ as spin B.The dipole-dipole relaxation contribution in ρ_T is from (spin D) $^{13}CO_i$, $^{1}H_i^\alpha$, $^{13}C_i^\alpha$. The dipole-dipole relaxation contribution in ρ_L is from (spin C) $^{15}N_i$, $^{13}CO_i$, $^{13}CO_{i-1}$, $^{1}H_{i+1}^N$, $^{1}H_{i+2}^N$, $^{1}H_i^\alpha$, $^{1}H_{i+1}^\alpha$, $^{1}H_{i+2}^\alpha$, $^{1}H_{i+3}^\alpha$, $^{1}H_{i+4}^\alpha$, $^{1}H_i^\beta$, $^{1}H_{i+1}^\beta$, $^{13}C_i^\alpha$, $^{13}C_{i-1}^\alpha$. The distance between nuclei were taken assuming the neighboring residues form an alpha helix.

2. Expression and purification of intrinsically disordered NFAT1$_{1-398}$ regulatory domain

The regulatory domain of human NFAT1 (residues 1–398), NFAT1$_{1–398}$, is expressed as a fusion with an N-terminal His-GB1 solubility tag in *E. coli* BL21 (DE3). The [U-^{15}N,^{13}C]-NFAT1$_{1-398}$ bacterial culture was grown using M9 minimal media containing 6 g/L Na_2HPO_4, 3 g/L KH_2PO_4, 0.5 g/L NaCl, 1 mM $MgSO_4$, and 0.1 mM $CaCl_2$ in H_2O supplemented with 4 g/L ^{13}C-glucose and 1 g/L of $^{15}NH_4Cl$. Cells were grown at 37 °C to an optical density of 0.8 measured at 600 nm wavelength. The temperature was dropped to 20 °C half an hour before inducing the expression by 1 mM isopropyl β-D-1-thiogalactopyranoside (IPTG). Cells continued to grow overnight at 20 °C before harvesting. The harvested cells were resuspended in 40 mL of 50 mM Tris·HCl (pH 8.0), 350 mM NaCl, 10 mM imidazole, and 5 mM β-mercaptoethanol (β-ME). The suspended cells were disrupted by sonication, and centrifuged for 40 min at 32,914 × g. The supernatant was collected and the insoluble fraction with cell debris was discarded. The supernatant was passed through gravity-flow affinity chromatography using 5 mL (10 mL of a 50% slurry) of Ni-NTA resin (Qiagen). After washing the resin with 40 mL of 50 mM Tris·HCl (pH 8.0), 350 mM NaCl, 40 mM imidazole, and 5 mM β-ME, the bound protein was eluted in an identical buffer containing 350 mM imidazole. The elution fraction was dialyzed against a buffer containing 30 mM Na_2HPO_4 (pH 6.7), NaCl (150 mM), and DTT (5

mM), and the His-GB1 solubility tag was cleaved using TEV protease. The digested $NFAT1_{1-398}$ and His-GB1 were separated and further purified using size exclusion chromatography (Superdex 75 10/300 GL; GE Healthcare Life Sciences).

We prepared two samples of $NFAT1_{1–398}$ for comparing $^{15}N^{TROSY}$ and $^{15}N^{D}$ detected experiments. We prepared the sample as described above and divided 1 ml samples to two 0.5 ml samples. Both were lyophilized and redissolved in protonated and deuterated buffer. The sample in deuterated buffer was left overnight for complete exchange of the $^{1}H^{N}$ with $^{2}H^{N}$.

3. Expression and purification of GB1

The Protein G B1 domain (GB1) was expressed as a fusion with an uncleavable C-terminal 6xHis tag in *E. coli* BL21 (DE3). The bacterial culture was grown in M9 minimal medium containing 6 g/L Na2HPO4, 3 g/L KH2PO4, 0.5 g/L NaCl, 2 mM MgSO4, and 0.1 mM CaCl2 in H2O supplemented with vitamin mix, trace elements, 2 g/L ^{13}C-glucose, and 1 g/L ^{15}NH4Cl. Cells were grown at 37 °C to a OD_{600} of 0.7. Subsequently, protein expression was induced through the addition of 0.5 mM isopropyl β-D-1-thiogalactopyranoside (IPTG) and carried out at 25 °C for 12 h. After being harvested, the cells were resuspended in 40 mL of lysis buffer (20 mM Tris-HCl pH 8.0, 150 mM NaCl, 10 mM imidazole) supplemented with 2.5 mM β-mercaptoethanol, lysozyme, benzonase and protease inhibitor (cOmplete EDTA-free, Roche). Cells were disrupted by sonication (power level 6, 5 min, 1 s on, 2 s off) and centrifuged at 37,000 x g for 45 min. The supernatant was collected and purified through affinity chromatography. To this end, it was incubated with 5 mL (10 mL of a 50% slurry) of pre-equilibrated Ni-NTA resin (Qiagen) for 1.5 h. The resin was washed with 50 mL of lysis buffer and subsequently eluted with 350 mM imidazole. The eluate was buffer exchanged and further purified by size exclusion chromatography (HiLoad pg Superdex 200 16/600) in NMR buffer (50mM sodium phosphate pH 6.5, 50mM NaCl). The final sample was concentrated to a final 1 mM for NMR spectroscopy, performed at 15 °C.

4. NMR experiments

All three-dimensional $^{15}N^{TROSY}$ NMR spectra were collected at 288 K using ~0.8 mM protein in 30 mM Na_2HPO4 (pH 6.7), 150 mM NaCl, and 5 mM DTT dissolved in 95% H_2O and 5% $^{2}H_2O$, using 5 mm NMR tube. For the backbone resonance assignment, ^{15}N-detected NMR spectra (haCACON, hacaCOCAN, hCBCACON, hCcaCON-TOCSY) were acquired on a Bruker Avance III spectrometer (Linux Operating system) operating at 800 MHz ^{1}H Larmor frequency and equipped with a triple-resonance cryogenic probe (TXO) in which the nitrogen

channel is on the inner coil and detected with cryogenically cooled preamplifiers. The haCACON (2D CO-N plane for confirming $^{15}N^{TROSY}$-detection), was recorded on a Bruker Avance I 500 MHz spectrometer with a TXO-style cryogenically cooled probe. The acquisition parameters are given in Table S1. We used the mixing time of 18 ms in the hCcaCON-TOCSY experiment using the FLOPSY[3] mixing sequence. All the three-dimensional spectra were acquired using NUS with 12.5% sampling of the Nyquist grid using Poisson Gap Sampling[4].

The acquisition parameters for comparing the ^{13}CO-^{15}N projections from $^{15}N^{D}$ detected haCACON, $^{15}N^{TROSY}$ haCACON and HNCO experiments are provided in Table S2.

The NUS spectra were reconstructed using hmsIST[5] and processed using NMRPipe. The spectra were analyzed with CcpNmr-Analysis (version 2.4.1)[6]. The average experimental time was ~ 4 days for each 3D experiment (see Table S1 for detailed acquisition parameters).

5. Assignment procedure

The assignment procedure used for $NFAT1_{1\text{-}398}$ uses the haCACON and hacaCOCAN spectra as complimentary experiments to find sequential connectivities between resonances.

Theoretically, the 2D CA-CO projection act in a similar manner as the H^{N}-N projection of regular ^{1}H-detected triple resonance experiments, and the ^{15}N dimension provides high resolution connections between peaks similarly to the HNCA and HNcoCA experiments' common ^{13}CA dimension (see **Fig. S9**). However, the CA-CO projection has low dispersion and is suboptimal to assign large IDRs.

We strongly recommend using the CA-N projection as a base for assignment routine given its high dispersion, high resolution in the ^{15}N dimension and large information content on amino acid and dipeptide types (see **Fig. 5**). An overlay of the 2D CA-N projections of the haCACON and hacaCOCAN experiments has all necessary information and will be enough to assign most small IDRs. For larger IDRs with more spectral corwding, the CO shifts in the third dimension will allow to distinguish ambiguous/overlapped peaks. The procedure is detailed below and schematized in **Fig. S9A**.

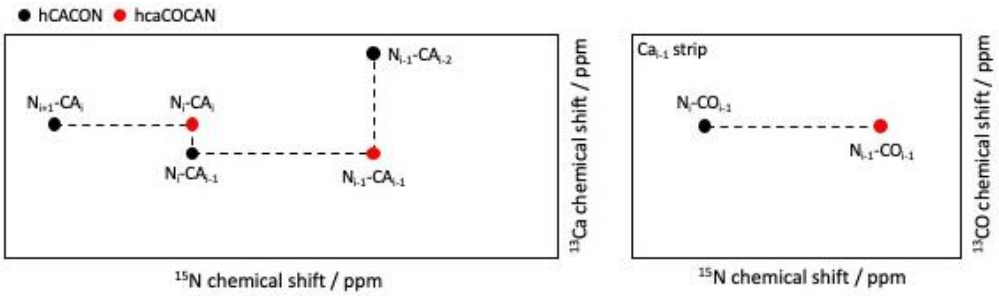

Figure S9A: **Assignment routine based on CA-N planes.** Black dots indicate hCACON peaks and red dots hcaCOCAN peaks. Sequential walk is shown for a tripeptide on the CA-N plane, the CO strip can help distinguish ambiguities or overlap.

<u>To find the previous residue in the sequence</u> :

- Select a (N_i, CA_i-1) correlation in the haCACON CA-N projection .
- In the hacaCOCAN CA-N projection, look for a signal at the same CA chemical shift, and read the N_{i-1} shift
- Look in the CA_{i-1} strip in the third dimension for a signal on the hacaCOCAN at the same CA chemical shift, read the N_{i-1} shift
- Look for a correlation on the haCACON CA-N projection at N_{i-1} to find N_{i-1}-CA_{i-2}

<u>To find the following residue in the sequence</u> :

- Select a correlation on the haCACON CA-N projection, encoding N_i-CA_{i-1}.
- Look for a signal on the hacaCOCAN CA-N projection at the same N chemical shift, read the CA_i shift
- Look for a correlation on the hCACON CA-N projection at CA_i to find N_{i+1}-CA_i
- Check that the CA_i strip on the third dimension has a signal at N_i-CO_{i-1} on the hcaCOCAN spectrum

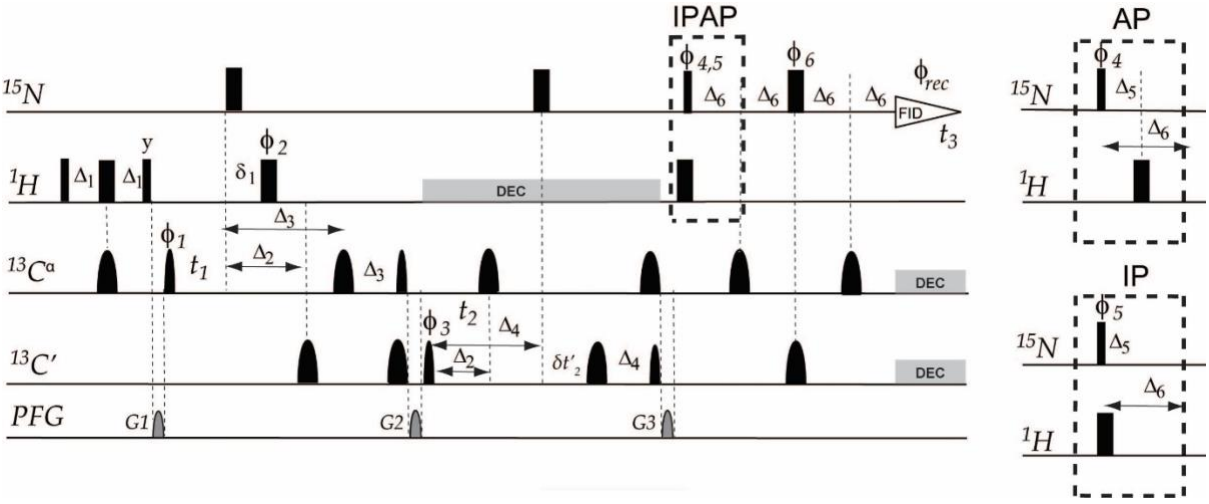

Figure S1: Pulse scheme for ^{15}N TROSY haCACON. Narrow and wide rectangles indicate π/2 and π non-selective pulses, respectively. Narrow and wide semi-ellipses indicate π/2 and π selective Gaussian cascade pulses (262 µs Q5-sebop and 202 µs Q3-surbop at 800 MHz), respectively. All pulses are applied along x unless otherwise specified. $\Delta_1 = 1/(4*J_{CH}) = 1.7$ ms, $\delta_1 = 1/(6*J_{CH}) = 1.1$ ms, $\Delta_2 = 1/(4*J_{CACO}) = 4.5$ ms, $\Delta_3 = 1/(2*J_{CC}) = 14.3$ ms, $\Delta_4 = 1/(4*J_{CON}) = 12.4$ ms, $\Delta_5 = 1/(4*J_{NH}) = 2.7$ ms, $\Delta_6 = \Delta_4/2 = 6.2$ ms, $t_1 = 0$ and $t_2 = 4.5$ ms. The $^{13}C^{\alpha}$ chemical shifts are evolved during t_1 in a constant time manner. The $^{13}C'$ chemical shifts are evolved during t_2 in a semi-constant time manner. Proton decoupling was achieved using WALTZ-16 (3.1 kHz). Adiabatic WURST decoupling was used for broadband ^{13}C decoupling (centered at 115 ppm, 2 ms, 30 kHz bandwidth and MLEV-16 supercycle). Phase sensitive spectrum in the $^{13}C(t_1)$ and $^{13}C(t_2)$ dimensions are obtained by incrementing the phases Φ_1 and Φ_3 in STATES-TPPI manner. Smoothened squared shaped pulsed-field gradients of duration 1 ms are applied on z-axis with G1 = 16.5 G/cm, G2 = 27.5 G/cm and G3 = 22 G/cm. All gradients are followed by recovery times of at least 200 µs. The following phase cycles are employed Φ_1 = (x,-x), Φ_2 = (x, x, -x, -x), Φ_3 = (8(x), 8(-x)), Φ_4 = (x, x, -x, -x), Φ_5 = (y, y, -y, -y), Φ_6 = (4(x), 4(-x)) and Φ_{rec} = (2(x, -x, -x, x), 2(-x, x, x, -x)).

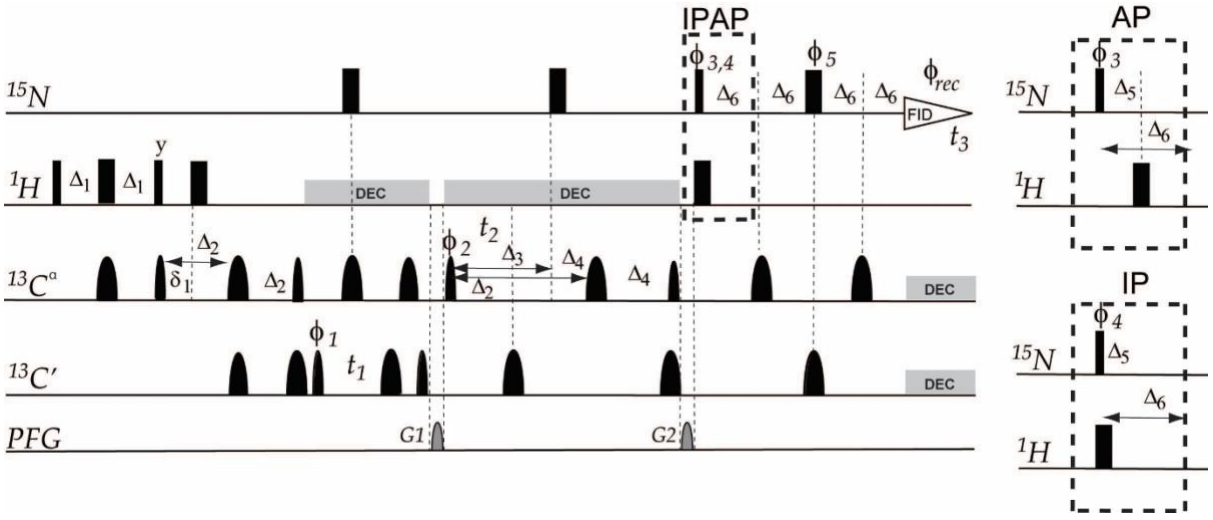

Figure S2: Pulse scheme for ^{15}N TROSY hacaCOCAN. Narrow and wide rectangles indicate π/2 and π non-selective pulses, respectively. Narrow and wide semi-ellipses indicate π/2 and π selective Gaussian cascade pulses (262 µs Q5-sebop and 202 µs Q3-surbop at 800 MHz), respectively. All pulses are applied along x unless otherwise specified. $\Delta_1 = 1/(4*J_{CH}) = 1.7$ ms, $\delta_1 = 1/(6*J_{CH}) = 1.1$ ms, $\Delta_2 = 1/(4*J_{CACO}) = 4.5$ ms, $\Delta_3 = 1/(2*J_{CC}) = 14.3$ ms, $\Delta_4 = 1/(4*J_{CON}) = 12.4$ ms, $\Delta_5 = 1/(4*J_{NH}) = 2.7$ ms, $\Delta_6 = \Delta_4/2 = 6.2$ ms and $t_2 = 4.5$ ms. The chemical shifts of ^{13}C' and $^{13}C^{\alpha}$ are evolved during t_1 and t_2 in real and constant time manner, respectively. Proton decoupling was achieved using WALTZ-16 (3.1 kHz). Adiabatic WURST decoupling was used for broadband ^{13}C decoupling (centered at 115 ppm, 2 ms, 30 kHz bandwidth and MLEV-16 supercycle). Phase sensitive spectrum in the $^{13}C(t_1)$ and $^{13}C(t_2)$ are obtained by incrementing the phases Φ_1 and Φ_3 in STATES-TPPI manner. Smoothened squared shaped pulsed-field gradients of duration 1 ms are applied on z-axis with G1 = 27.5 G/cm and G2 = 22 G/cm. All gradients are followed by recovery times of at least 200 µs. The following phase cycles are employed Φ_1 = (x, -x), Φ_2 = (8(x), 8(-x)), Φ_3 = (x, x, -x, -x), Φ_4 = (y, y, -y, -y), Φ_6 = (4(x), 4(-x)) and Φ_{rec} = (2(x, -x, -x, x), 2(-x, x, x, -x)).

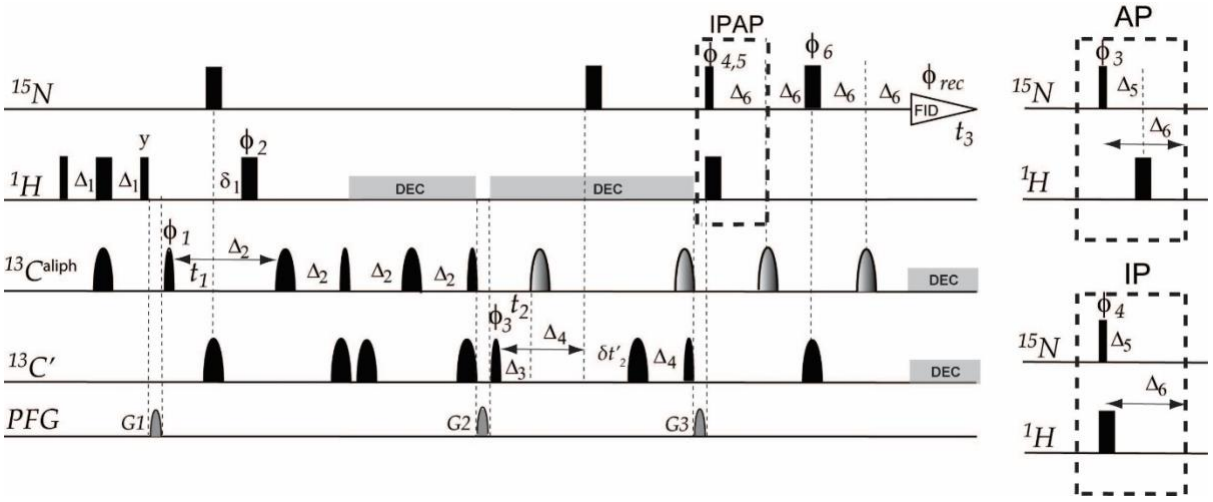

Figure S3: Pulse scheme for ^{15}N TROSY hCBCACON. Narrow and wide rectangles indicate π/2 and π non-selective pulses, respectively. Narrow and wide semi-ellipses indicate π/2 and π selective Gaussian cascade pulses (262 µs Q5-sebop and 202 µs Q3-surbop at 800 MHz), respectively. All pulses are applied along x unless otherwise specified. The gradient shaded pulses are applied with $^{13}C^{\alpha}$ carrier frequency (52 ppm) while other pulses are applied $^{13}C^{aliphatic}$ carrier frequency (42 ppm). The delays $\Delta_1 = 1/(4*J_{CH}) = 1.7$ ms, $\delta_1 = 1/(6*J_{CH}) = 1.1$ ms, $\Delta_2 = 1/(8*J_{CC}) = 3.6$ ms, $\Delta_3 = 1/(4*J_{CACO}) = 4.5$ ms, $\Delta_4 = 1/(4*J_{CON}) = 12.4$ ms , $\Delta_5 = 1/(4*J_{NH}) = 2.7$ ms, $\Delta_6 = \Delta_4/2 = 6.2$ ms. The chemical shifts of $^{13}C^{\alpha/\beta}$ and $^{13}C'$ and are evolved during t_1 and t_2 in constant and semi-constant time manner, respectively. Proton decoupling was achieved using WALTZ-16 (3.1 kHz). Adiabatic WURST decoupling was used for broadband ^{13}C decoupling (centered at 115 ppm, 2 ms, 30 kHz bandwidth and MLEV-16 supercycle). Phase sensitive spectrum in the $^{13}C(t_1)$ and $^{13}C(t_2)$ are obtained by incrementing the phases Φ_1 and Φ_3 in STATES-TPPI manner. Smoothened squared shaped pulsed-field gradients of duration 1 ms are applied on z-axis with G1 = 16.5 G/cm, G2 = 27.5 G/cm and G3 = 22 G/cm. All gradients are followed by recovery times of at least 200 µs. The following phase cycles are employed Φ_1 = (x, -x), Φ_2 = (x, x, -x, -x), Φ_3 = (8(x), 8(-x)), Φ_4 = (x, x, -x, -x), Φ_5 = (y, y, -y, -y), Φ_6 = (4(x), 4(-x)) and Φ_{rec} = (2(x, -x, -x, x), 2(-x, x, x, -x)).

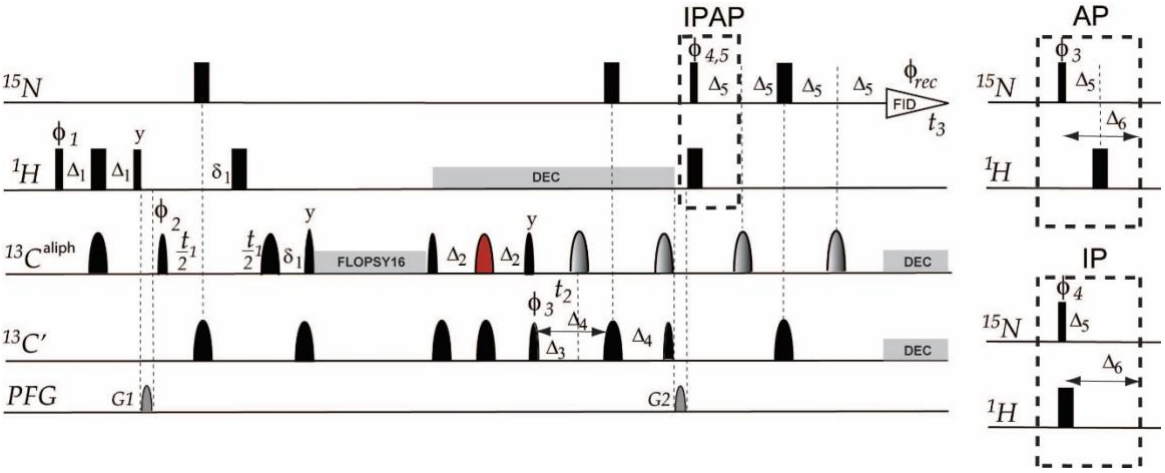

Figure S4: Pulse scheme for ^{15}N TROSY hCCCON-TOCSY. Narrow and wide rectangles indicate π/2 and π non-selective pulses, respectively. Narrow and wide semi-ellipses indicate π/2 and π selective Gaussian cascade pulses (262 µs Q5-sebop and 202 µs Q3-surbop at 800 MHz), respectively. All pulses are applied along x unless otherwise specified. The gradient shaded pulses are applied with $^{13}C^{\alpha}$ carrier frequency (52 ppm) while other pulses are applied $^{13}C^{aliphatic}$ carrier frequency (42 ppm). The red colored selective pulse is applied with $^{13}C^{\alpha}$ carrier frequency and is a C^{α} selective Q3surbop/750 µs pulse. $\Delta_1 = 1/(4*J_{CH}) = 1.7$ ms, $\delta_1 = 1/(6*J_{CH}) = 1.1$ ms, $\Delta_2 = 1/(8*J_{CC}) = 3.6$ ms, $\Delta_3 = = 1/(4*J_{CACO}) = 4.5$ ms , $\Delta_4 = 1/(4*J_{CON}) = 12.4$ ms, $\Delta_5 = 1/(4*J_{NH}) = 2.7$ ms, $\Delta_6 = \Delta_4/2 = 6.2$ ms. Total correlation spectroscopy is achieved through a FLOPSY [3] sequence applied for 18 ms at a field of 3.2 kHz. The chemical shifts of $^{13}C^{aliphatic}$ and $^{13}C'$ are evolved during t_1 and t_2 in real time and constant time manner, respectively. Proton decoupling was achieved using WALTZ-16 (3.1 kHz). Adiabatic WURST decoupling was used for broadband ^{13}C decoupling (centered at 115 ppm, 2 ms, 30 kHz bandwidth and MLEV-16 supercycle). Phase sensitive spectrum in the $^{13}C(t_1)$ and $^{13}C(t_2)$ dimensions are obtained by incrementing the phases Φ_1 and Φ_3 in STATES-TPPI manner. Smoothened squared shaped pulsed-field gradients of duration 1 ms are applied on z-axis with G1 = 27.5 G/cm and G2 = 22 G/cm. All gradients are followed by recovery times of at least 200 µs. The following phase cycles are employed Φ_1 = (8(x), 8(-x)), Φ_2 = (x, x, -x, -x), Φ_3 = (4(x), 4(-x)), Φ_4 = (x, x, -x, -x), Φ_5 = (y, y, -y, -y) and Φ_{rec} = (2(x, -x, -x, x), 2(-x, x, x, -x)).

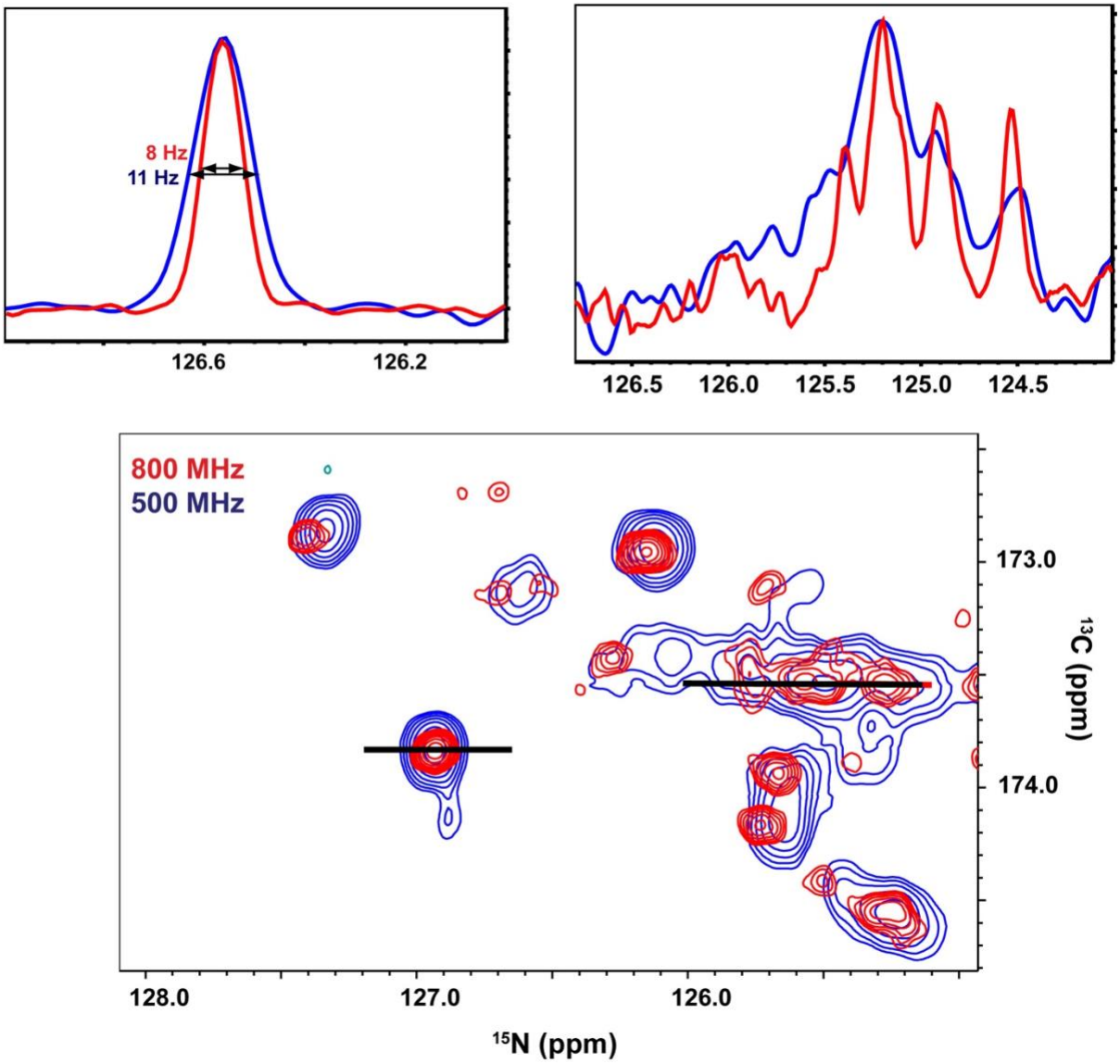

Figure S5: **Comparison of TROSY effects at 11.74 T and 18.79 T.** The bottom panel shows a section of 2D ^{13}CO-^{15}N projection of haCACON spectrum measured at two field strengths with $^{15}N^{H}$-TROSY spin state selection. Selected 1D slices are displayed on top for regions highlighted with black horizontal lines in the projection. $^{15}N^{H}$-TROSY linewidth is narrower for magnetic field 18.79 T (800 MHz) when compared to 11.74 T (500 MHz). The measured value of linewidths are shown for left panel.

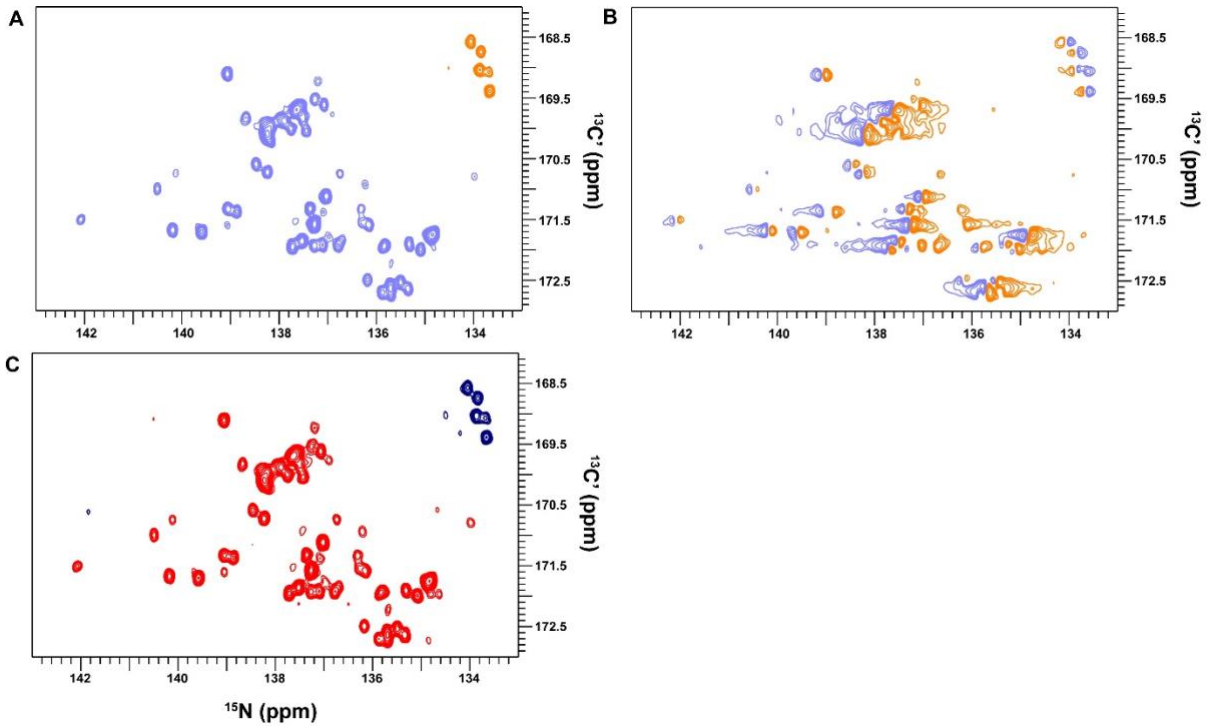

Figure S6: Example of 2D ^{13}CO-^{15}N projection of haCACON for prolines. The proline residues are singlet peaks in both the in-phase (A) and anti-phase (B) spectra. The peak phases are out of phase by 90 in the anti-phase spectrum and can be corrected with a zero order phase correction (C) before summing both datasets.

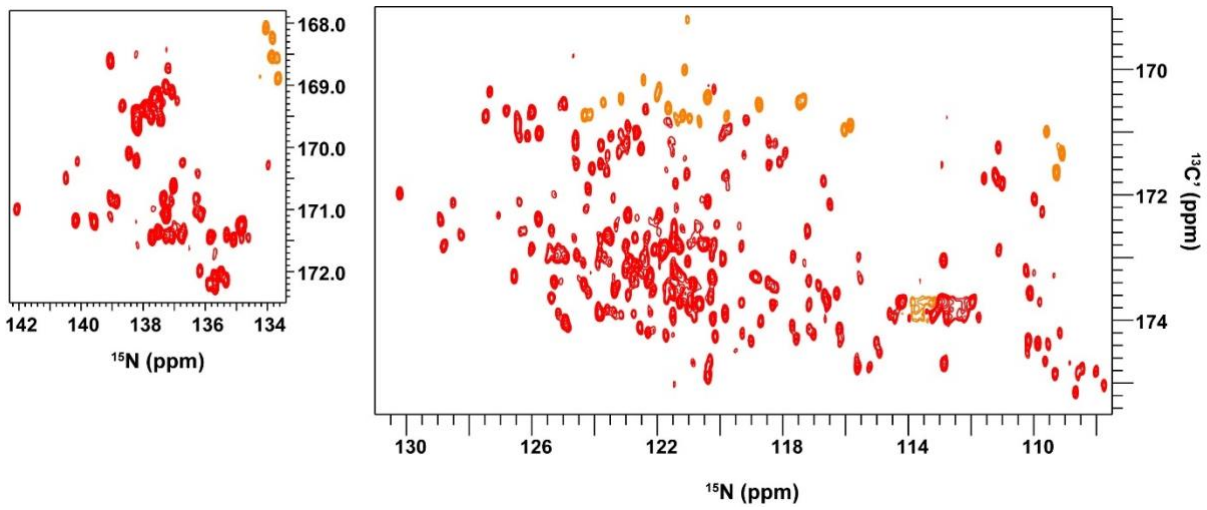

Figure S7: 2D ^{13}CO-^{15}N projection of haCACON. The left hand panel shows the Proline chemical shift region of the spectrum, which is phased separately. The ^{13}C' and ^{15}N chemical shift of i-1 and i residue, respectively, are correlated in this spectrum.

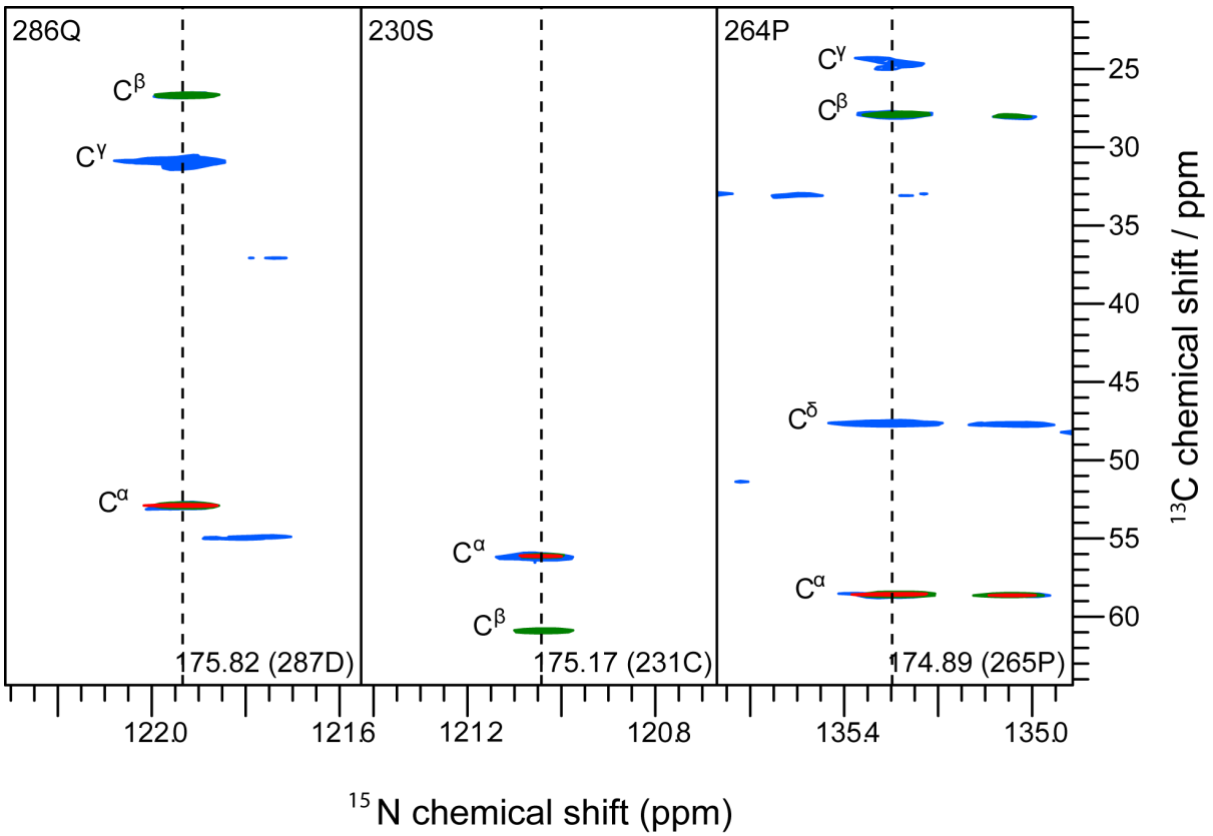

Figure S8: **Examples of strips extracted from 3D experiments.** Three examples of strip plots from overlay of haCACON (red), hCBCACON (green) and hCCCON-TOCSY (blue) spectra of $NFAT1_{1-398}$ are shown. The strips are taken using the $^{13}C'$ and ^{15}N chemical shifts common across all three experiments.

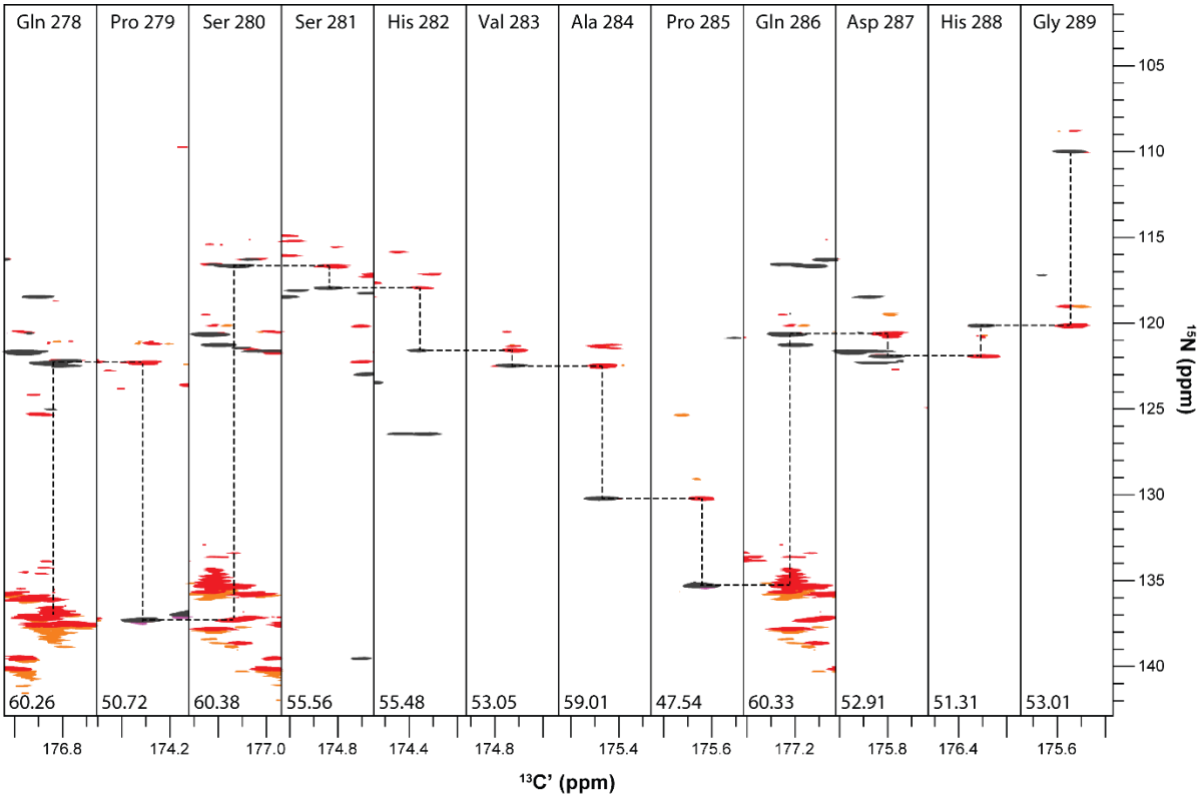

Figure S9: A walk through the hacaCOCAN spectra strips for resonance assignment. Three-dimensional strip plot overlay of hcaCOCAN (red) and hCACON (grey) for NFAT1$_{1\text{-}398}$. The strips are taken using the common ^{13}C' and ^{13}C$^{\alpha}$ chemical shifts of both experiments. The assignment stretch shown contain two prolines.

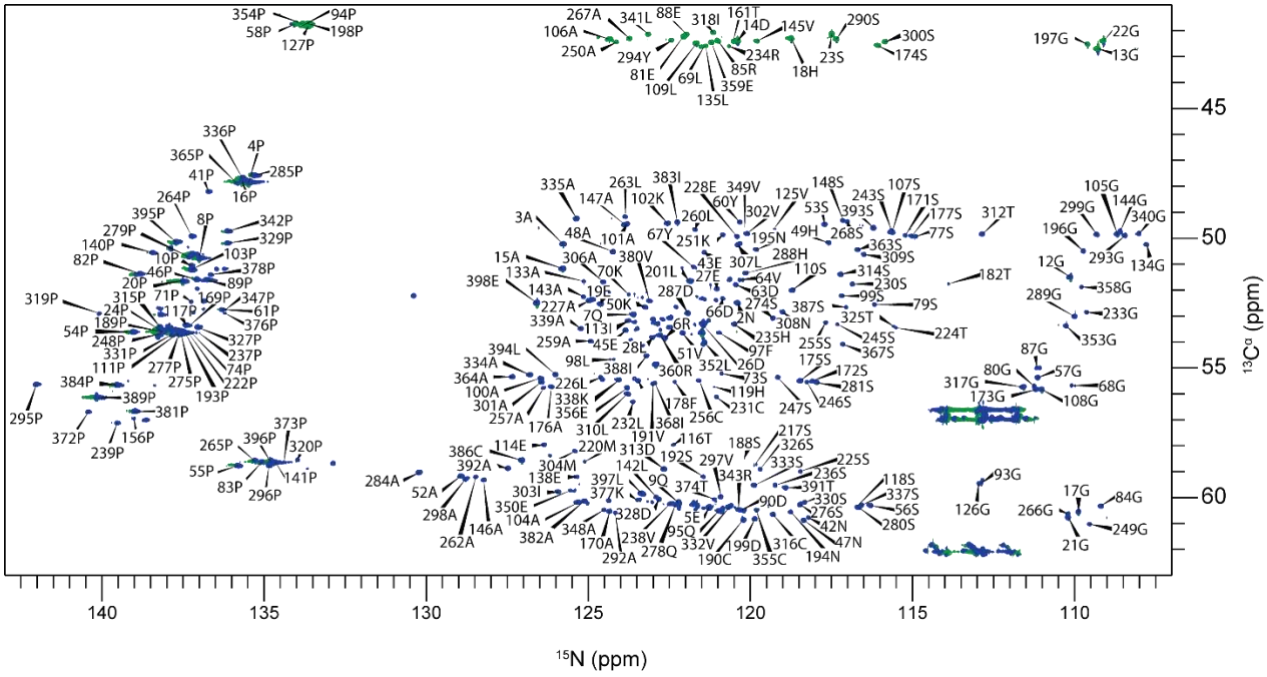

Figure S10: **Sequence specific resonance assignments of NFAT1$_{1\text{-}398}$.** The peaks are marked with residue number and amino acid type of $^{15}N_i$ residue in the $^{13}C^{\alpha}_{i-1}$ and $^{15}N_i$ correlation in the 2D CA-N projection of hCACON spectrum.

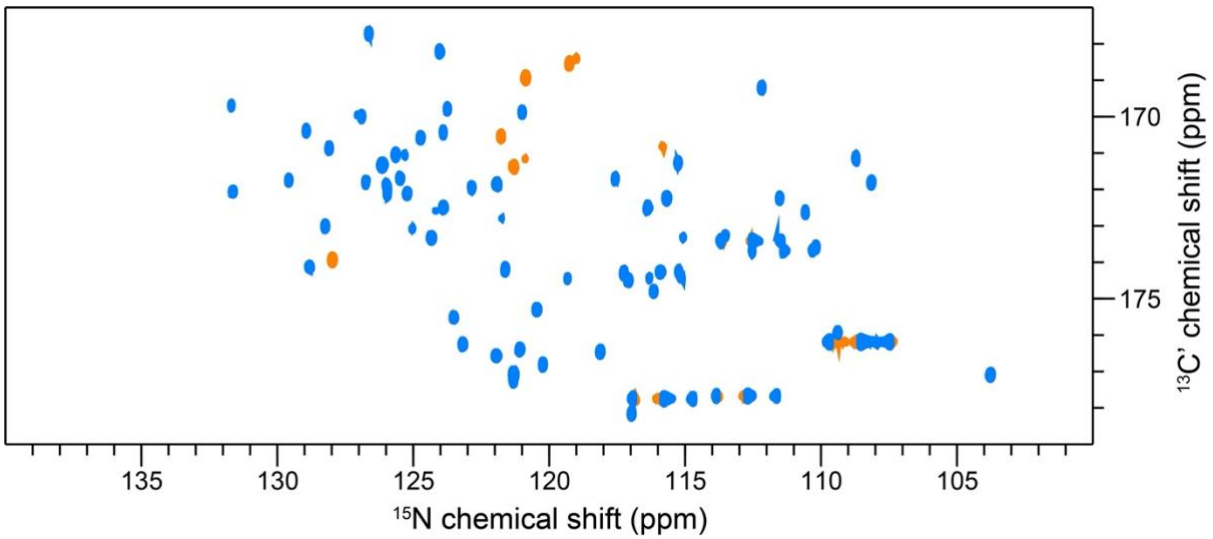

Figure S11: **2D CO-N plane of hacaCON 3D experiment for GB1 at 15 °C.** The expected number of peaks (~90) is visible, including the 7 peaks corresponding to Gly-X dipeptides in negative contours (orange).

Table S1 Acquisition parameters for the NMR experiments reported in this paper.

	haCACON			**hacaCOCAN**			**hCBCACON**			**hCCCON (TOCSY)**		
Parameters	$^{13}C^{\alpha}$	^{13}CO	^{15}N	^{13}CO	$^{13}C^{\alpha}$	^{15}N	$^{13}C^{aliph}$	^{13}CO	^{15}N	$^{13}C^{aliph}$	^{13}CO	^{15}N
Number of scans	64			80			80			80		
Number of dummy scans	32			32			32			32		
Pre-acquisition delay (μs)	18			18			18			18		
Recycle delay (sec)	1.2			1.2			1.2			1.2		
Acquisition time (ms)	13.4	19.9	189	19.9	16.6	189	6.6	19.9	189	6.6	19.9	189
# Complex points (Real + Imaginary) 'TD' 12.5% of TD are non-uniform sampled	140	96	1536	96	160	1536	160	96	1536	160	96	1536
Spectral Width (ppm)	24	12	50	12	24	50	60	12	50	60	12	50
Transmitter Offset (ppm)	52	172.5	122	172.5	52	122	42	172.5	122	42	172.5	122

Table S2 Acquisition parameters for the NMR experiments reported in this paper.

	$^{15}N^{TROSY}$ haCACON			**$^{15}N^{D}$ haCACON**			**HNCO**		
Parameters	$^{13}C^{\alpha}$	^{13}CO	^{15}N	$^{13}C^{\alpha}$	^{13}CO	^{15}N	^{13}CO	^{15}N	^{1}H
Number of scans	128			256			16		
Number of dummy scans	32			32			32		
Pre-acquisition delay (μs)	18			18			10		

Recycle delay (sec)	1.2			1.2			1.2		
Acquisition time (ms)	NA	53	126	NA	26.5	126	26.5	22.8	91.7
# Complex points (Real + Imaginary) TD	1	256	1024	1	128	1024	128 (12.5% of TD non-uniform sampled)	96	2048
Spectral Width (ppm)	NA	12	50	NA	12	50	12	26	14
Transmitter Offset (ppm)	NA	173	125	NA	173	125	173	119	4.7

References

1. Wagner, G. NMR relaxation and protein mobility. *Curr. Opin. Struct. Biol.* **3**, 748-754 (1993).
2. Zhu, G. & Yao, X. TROSY-based NMR experiments for NMR studies of large biomolecules. *Progress in Nuclear Magnetic Resonance Spectroscopy* **52**, 49-68 (2008).
3. Kadkhodaie, M., Rivas, O., Tan, M., Mohebbi, A. & Shaka, A.J. Broadband homonuclear cross polarization using flip-flop spectroscopy. *Journal of Magnetic Resonance (1969)* **91**, 437-443 (1991).
4. Hyberts, S.G., Takeuchi, K. & Wagner, G. Poisson-gap sampling and forward maximum entropy reconstruction for enhancing the resolution and sensitivity of protein NMR data. *J Am Chem Soc* **132**, 2145-7 (2010).
5. Hyberts, S.G., Milbradt, A.G., Wagner, A.B., Arthanari, H. & Wagner, G. Application of iterative soft thresholding for fast reconstruction of NMR data non-uniformly sampled with multidimensional Poisson Gap scheduling. *Journal of biomolecular NMR* **52**, 315-27 (2012).
6. Vranken, W.F. et al. The CCPN data model for NMR spectroscopy: development of a software pipeline. *Proteins* **59**, 687-96 (2005).